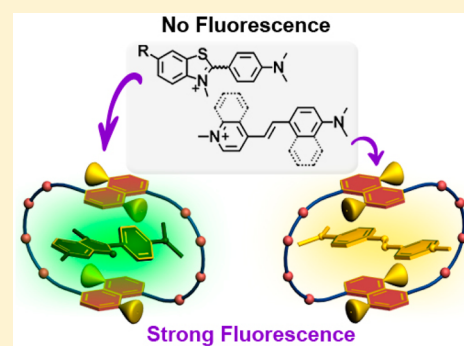


Rigid Organization of Fluorescence-Active Ligands by Artificial Macrocyclic Receptor to Achieve the Thioflavin T-Amyloid Fibril Level Association

Ying-Ming Zhang,[†] Xu-Jie Zhang,[†] Xiufang Xu,[†] Xiao-Ning Fu,[†] Hong-Biao Hou,[†] and Yu Liu^{*,†,‡}[†]Department of Chemistry, State Key Laboratory of Elemento-Organic Chemistry, Nankai University, Tianjin 300071, P. R. China[‡]Collaborative Innovation Center of Chemical Science and Engineering (Tianjin), Tianjin 300071, P. R. China

S Supporting Information

ABSTRACT: The push–pull molecules with an intramolecular charge transfer from donor to acceptor sides upon excitation exhibit a wide variety of biological and electronic activities, as exemplified by the *in vivo* fluorescence imaging probes for amyloid fibrils in the diagnosis and treatment of amyloid diseases. Interestingly, the structurally much simpler bis(4,8-disulfonato-1,5-naphtho)-32-crown-8 (DNC), in keen contrast to the conventional macrocyclic receptors, was found to dramatically enhance the fluorescence of twisted intramolecular charge-transfer molecules possessing various benzothiazolium and stilbazolium fluorophores upon complexation. Spectroscopic and microcalorimetric titrations jointly demonstrated the complex structures and the interactions that promote the extremely strong complexation, revealing that the binding affinity in these artificial host–guest pairs could reach up to a nearly 10^7 M⁻¹ order of magnitude in water, and the sandwich-type complexation is driven by electrostatic, hydrophobic, π -stacking, and hydrogen-bonding interactions. Quantum chemical calculations on free molecules and their DNC-bound species in both the ground and excited states elucidated that the encapsulation by DNC could greatly deter the central single and double chemical bonds from free intramolecular rotation in the singlet excited state, thus leading to the unique and unprecedented fluorescence enhancement upon sandwich-type complexation. This complexation-induced structural reorganization mechanism may also apply to the binding of other small-molecule ligands by functional receptors and contribute to the molecular-level understanding of the receptor–ligand interactions in many biology-related systems.



INTRODUCTION

Receptor–ligand binding is regarded as one of the most ubiquitous and diverse processes in biochemical events, such as the transportation of oxygen by hemoglobin and the complexation of DNA with histone in higher organisms.^{1–3} The activation or inhibition of a receptor can be driven by the capture of an endogenous or exogenous ligand and starts with a conformational change followed by a biological chain of reactions, e.g., the light-induced signal transduction by natural photosensory receptors.^{4,5} The “induced-fit” mechanism on enzyme catalysis has pointed out that the tight shape complementarity plays a critical role in the binding process,^{6,7} and consequently, the structural rearrangements that can accompany receptor–ligand binding have been comprehensively explored over the past few decades.^{8–14} Regardless of the significant progress on the experimental evidence and theoretical prediction to illustrate the receptor–ligand binding behaviors with continuously increasing accuracy and specificity, mapping the structure–activity relationships in receptor–ligand systems always requires detailed knowledge of the nature and origins of changes in chemical and physical states of the participating ligands and receptors, but there is a relative paucity of studies until recently on the magnitude and

prevalence of spatial organization upon receptor–ligand complexation. For instance, thioflavin T (G1, Figure 1), a benzothiazole-based cationic dye molecule, is unanimously accepted as the “gold standard” and potent fluorescent biomarker for selectively staining and identifying the probe–target association with amyloid fibrils (aggregates of proteins that possess 39–43 amino acid residue peptide).^{15,16} Despite the extensive studies on the photophysical properties of G1, however, the mechanism by which the binding of G1 toward the nanopores of amyloid fibrils that leads to a dramatic fluorescence enhancement remains largely unknown, and the literature reports are even contradictory at times.¹⁷ Nevertheless, the most convincing hypothesis, which was comprehensively verified by spectroscopy measurements and X-ray crystallography analyses, has implied that the inhibition of the rotation around a single C–C bond in G1 is the crucial and basic factor to govern the specific recognition toward amyloid fibrils.^{18,19}

Received: March 14, 2016

Revised: April 5, 2016

Published: April 5, 2016

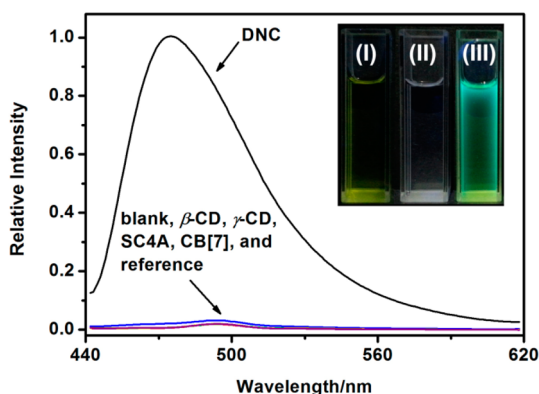


Figure 1. Fluorescence spectra of G1 in the presence and absence of DNC and other representative macrocyclic receptors. Fluorescence spectral changes upon addition of DNC, β -CD, γ -CD, SC4A, CB[7] and disodium 1,5-naphthalenedisulfonate (reference compound) were monitored under comparable conditions in water at 25 °C; [G1] = 1.0×10^{-6} M, [DNC] = [β -CD] = [γ -CD] = [SC4A] = [CB[7]] = 5.0×10^{-6} M, [reference] = 1.0×10^{-5} M; excitation wavelength = 425 nm. Inset: photographs of the solutions of G1 (I), DNC (II), and G1CDNC complex (III) irradiated under UV light.

To date, supramolecular methodology has been proven as an alternative and even a more powerful strategy to create new photophysical and biomedical properties through elaborately modulating the intermolecular noncovalent interactions.^{20–23} More excitingly, supramolecularly assembled entities have provided numerous structurally and kinetically well-defined and well-characterized model systems to simplify and mimic the realistic prototype in the macroscopic and microscopic world, which allow us to describe a more detailed picture of molecular recognition mechanism in biological systems.^{24,25} We report here a unique fluorescence enhancement of push–pull molecules (G1–G6) upon binding to bis(4,8-disulfonato-1,5-naphtho)-32-crown-8 (DNC) in water, with the aim of gaining mechanistic implications for the recognition-induced conformational changes upon artificial receptor–ligand binding (Chart 1). As a negatively charged synthetic receptor with a flexible and nonpreorganized structure, DNC bears the essential structural features of the three-dimensional hydrophobic “pocket” of some biomacromolecules, thus making such water-soluble crown ether a promising candidate for mimicking the biological receptor–ligand recognition process at a molecular resolution. In our previous work, we have established that sulfonated crown ethers and their higher homologues can effectively encapsulate diverse types of organic cations in its

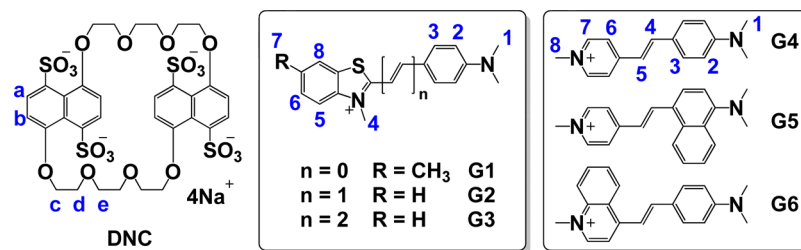
hydrophobic cavity through multiple noncovalent interactions, i.e., the hydrogen-bonding interconnection with polyether chains, the electrostatic attraction with sulfonate sites, and the aromatic stacking contact with disulfonatophthalene planes.^{26–28} All of these characteristic interactions are expected to operate as the main driving forces in the specific binding of ligands with proteins and many other biomacromolecular assemblies,²⁹ and hence the results of this study will significantly promote our molecular-level understanding of the receptor–ligand binding in relevant biological systems.

RESULTS AND DISCUSSION

Host Selectivity with Push–Pull Molecules.

Crown ether DNC sodium salt was prepared by our previous method.³⁰ Two types of monocationic ligands (benzothiazolium and stilbazolium salts) were synthesized according to the reported methods,^{31,32} in which the counterion was exchanged to chloride ion as to improve their water solubility. Fluorescence spectral behavior of G1 was preliminarily examined in water with and without added DNC, where the excitation wavelength was set at 425 nm to avoid any light absorption by DNC (Figure S1 in the Supporting Information). As can be seen from Figure 1, the fluorescence intensity of G1 showed a sudden leap by a factor of 140 upon addition of DNC, accompanied by a large hypochromatic shift from 495 to 472 nm, which is contributed to the visible emission from the charge transfer (CT) state to the locally excited (LE) state. This dramatic fluorescence enhancement is comparable to the thioflavin T–amyloid fibrils level association¹⁷ and indicates the close intermolecular communication between DNC and G1 in water. In keen contrast, none of the other representative macrocyclic receptors, including β - and γ -cyclodextrins (β - and γ -CDs), *p*-sulfonatocalix[4]arene (SC4A) and cucurbit[7]uril (CB[7]), showed such behaviors under the same experimental condition.^{33,34} This specific binding of G1 by DNC could be detected also by the naked eyes, since neither G1 nor DNC is fluorescent (see photographs I and II in Figure 1, inset), but an equimolar mixture of the two components instantly became highly fluorescent to emit intense yellowish green light upon exposure to UV light (see photograph III in Figure 1, inset). In a control experiment, no spectral change of G1 was observed in the presence of disodium 1,5-naphthalenedisulfonate added as a reference compound, indicating that the electrostatic attraction is not sufficient to form a host–guest complex and the macrocyclic structure of DNC is indispensable to entrap G1 in its preorganized π -electron-rich cavity (Figure S2 in the Supporting Information). This excellent host selectivity of

Chart 1. Chemical Structures of DNC, Benzothiazolium Salts (G1–G3), Stilbazolium Salts (G4–G6), and Proton Designation in G1 and G4^a



^aThe counterion in all guest molecules is Cl[−]. Two 4,8-disulfonatophthalene units are covalently lined together at the 1- and 5-positions with trioxyethylene chains in host DNC, while two push-pull aromatic planes can interact with each other via a π -conjugated spacer in guests G1–G6.

DNC toward G1 prompted us to hypothesize that tetrasulfonated crown ethers could be utilized as a versatile candidate to substantially improve the inherent spectroscopic performance of some specific ligands through the synergetic supramolecular cooperativity.

With this in mind, the ligand structures were extended from the turn-on fluorescence biomarker thioflavin T (G1) to various benzothiazolium and stilbazolium salts (G2–G6).^{35–37} All the selected guest molecules are dipolar push–pull organic chromophores, in which the strong electron-donor and electron-acceptor groups positioned at the opposite ends of a π -conjugation path.³⁸ It is believed that the intensive positive charges in the heteroaromatic center of G1–G6 not only act as the electron-deficient moiety to achieve an optimal donor–acceptor combination but also facilitate the electrostatic attraction with negatively charged sulfonate groups in DNC, while their aromatic skeleton may simultaneously increase the π -stacking probability with naphthyl rings in DNC. Therefore, the formation and structural features of push–pull molecules G1–G6 upon complexation with DNC were qualitatively studied by UV/vis and ¹H NMR spectral examinations. As shown in Figure 2, the absorption peak of G1 centered at 412

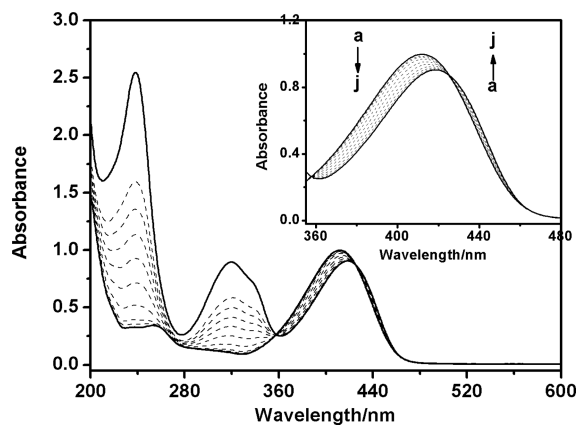


Figure 2. UV/vis spectral changes of G1 upon addition of DNC to form binary complexes. The spectral changes were recorded in water at 25 °C; [G1] = 4.0×10^{-5} M, [DNC] = $0-8.0 \times 10^{-5}$ M (from line a to j). Inset: the magnified spectra in the range from 360 to 480 nm, showing the isosbestic point at 425 nm.

nm was gradually shifted to 419 nm with an isosbestic point at 425 nm upon stepwise addition of DNC of up to 2 equiv, indicating the simple one-step transformation from free G1 to G1CDNC complex in aqueous solution. Similarly, the UV/vis absorption of stilbazolium guest G4 gradually decreased upon addition of DNC in the range of 370–550 nm, but no obvious isosbestic point was observed in the G4CDNC complex at long-wavelength region (Figure S3 in the Supporting Information).

¹H NMR Titration. Furthermore, the structural features of the obtained binary complexes were elucidated from the chemical shift changes of the ¹H NMR spectra. As can be seen from Figure 3, the dimethylaniline's H_{1–2} protons and the benzothiazole's H₇ proton (see Chart 1), which are located at the both ends of G1, are shifted to the low field by 0.12, 0.22, and 0.03 ppm, respectively, upon complexation. In comparison, the remaining aromatic and H₄ protons, all of which are located in the central part of G1 molecule, show pronounced upfield shifts of up to 0.26 ppm upon complexation. In addition, the

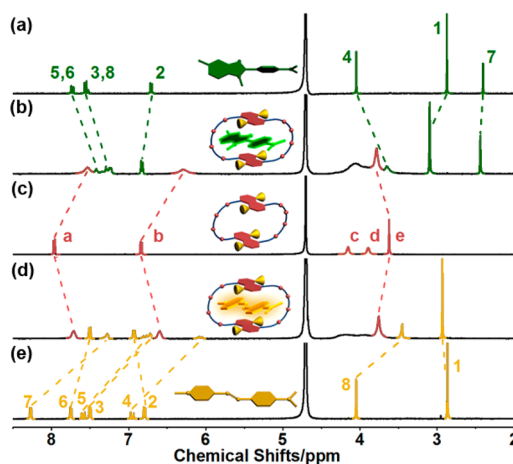


Figure 3. Chemical shift changes of G1 and G4 with DNC upon complexation. ¹H NMR spectra of (a) G1, (b) G1CDNC, (c) DNC, (d) G4CDNC, and (e) G4 were recorded in D₂O at 25 °C; [DNC] = [G1] = [G4] = 2.0×10^{-3} M.

DNC's aromatic a and b protons show much larger upfield shifts of 0.43 and 0.56 ppm, respectively, and the signals are significantly broadened upon complexation with G1. Similar broadening is seen also for the oxyethylene proton signals c–e with nominal chemical shift changes (Figure 3b). In contrast, although a simple pattern of sharp peaks for the individual G2–G3 was observed, the resonance signals of their corresponding supramolecular complexes were drastically broadened and suffered pronounced downfield shifts as a result of the tight encapsulation in the crown ether's cavity (Figure S4 in the Supporting Information). All the phenomena may be indicative of a slow exchange dynamics due to a relatively high binding strength of DNC with the examined push–pull guests in water, which is further validated by the fluorescence titration experiments, as described below.

In the case of stilbazolium salt G4, the corresponding chemical shift changes exhibited a similar tendency upon addition of DNC; that is, the pyridinium ring and double-bond protons in G4 (H_{3–8}) exhibit dramatic upfield shifts, which were mainly attributed to mutual strong diamagnetic shielding between the naphthalene and pyridinium sites. Also, the rest protons in G4 (H_{1–2}) gave downfield shifts upon complexation with DNC, suggesting that the dimethylaniline part was mostly located outside the macrocyclic ring. These ¹H NMR spectroscopic observations were in good agreement with our previous study that the supramolecular complexation with tetrasulfonated crown ethers always moves the proton signals of accommodated guest molecule to the higher field but those located outside the cavity to the lower field.²⁶ Similarly, the molecular binding behaviors could be also deduced from the ¹H NMR spectra of G5CDNC and G6CDNC complexes (Figure S5 in the Supporting Information). Overall, the above-mentioned contrasting NMR spectral behaviors of the peripheral and central protons of push–pull ligands upon complexation with DNC indicate that the aromatic core of guest molecules is firmly sandwiched by DNC's two naphthalene moieties as a consequence of the combined effects of the π -stacking, electrostatic attraction, and the C–H...O hydrogen-bonding with the ether oxygen in the linker as indicated by the quantum chemical calculations (*vide infra*), leaving the dimethylamino group and its periphery protons in the deshielding area of the naphthalenes in DNC.

Furthermore, rotating-frame Overhauser effect spectroscopy (ROESY) experiments provided more detailed structural information about the G1CDNC complex. In the ROESY spectrum shown in Figure S6 (the Supporting Information), cross-peak A is assignable to the nuclear Overhauser enhancement (NOE) correlation between the G1's H₂ proton and the DNC's a proton and the cross-peaks B and C to the NOE correlation between one of the G1's central aromatic protons and the DNC's H_c proton on the linker. Combining these ROESY results with the aforementioned chemical shift changes upon complexation, we can conclude that the guest molecules are tightly packed between the two naphthalene rings of DNC to form a sandwich-type complex in water, and this binding mode enables the dramatic enhancement of G1–G6 fluorescence, the mechanism of which will be discussed below.

Fluorescence Spectroscopic Titration. The association constants (*K*) of G1–G6 with DNC were determined by fluorescence spectral titration at relatively low concentrations.^{39,40} First, the binding stoichiometry was determined by the Job analysis at a fixed total concentration of host and guest molecules. As shown in Figure S7, the fluorescence intensity changes (ΔF) were plotted against the molar fraction of G1 to give a peak at a molar fraction of 0.5, indicating 1:1 stoichiometry for the G1–DNC complexation. In addition, the formation of a 1:1 complex was further confirmed by electrospray ionization–mass spectrometry (ESI-MS). The corresponding molecular ion peaks for all the 1:1 binary complexes could be observed in Figures S8–S13 (Supporting Information).

Then, the fluorescence spectral titration of G1–G6 with DNC was performed in water at 25 °C to give the results shown in Figures 4 and S14 (Supporting Information). It is noteworthy that the complexation of DNC can consistently induce an appreciable fluorescence enhancement with all the selected push–pull molecules, here again corroborating the power of preorganized macrocyclic ring of DNC in the regulation of photophysical properties of organic dyes. Moreover, the nonlinear least-squares fit of the intensity changes (ΔF), assuming the 1:1 complex stoichiometry, afforded the association constant (*K*) as high as $5.02 \times 10^6 \text{ M}^{-1}$ in the G2CDNC complex (Figure 4a). Using the same fluorescence titration method, the *K* value between G6 and DNC under a neutral condition was calculated to be $2.25 \times 10^6 \text{ M}^{-1}$ (Figure 4b). For a comparison purpose, all the *K* values derived from fluorescence spectroscopic titrations in the complexation of DNC with guests G1–G6 were listed in Table S1. It can be seen that the binding strength was mostly located in the range of 10^6 M^{-1} order of magnitude, except the one of DNC with G2 and G3 bearing a broader aromatic conjugation to reach the highest value of $5.02 \times 10^6 \text{ M}^{-1}$, which exceeds the values reported for synthetic host–guest systems (typically 10^1 – 10^6 M^{-1} ; mean at *ca.* 3000 M^{-1}) and is comparable to those for antigen–antibody systems (10^7 – 10^9 M^{-1}).⁴¹ This phenomenon probably originates from a closer and compacter aromatic π -stacking interaction to achieve a greater size–fit efficiency in the obtained host–guest complexes.

More crucially, the time-resolved fluorescence studies under the comparable conditions demonstrated that the complexation with DNC significantly elongated the fluorescence lifetime of G1 from several picoseconds to 0.5 ns (Figure S15 in the Supporting Information),⁴² which is likely due to the electronic and structural effects of sandwich complexation as well as the protection from the deactivating solvent attacks.

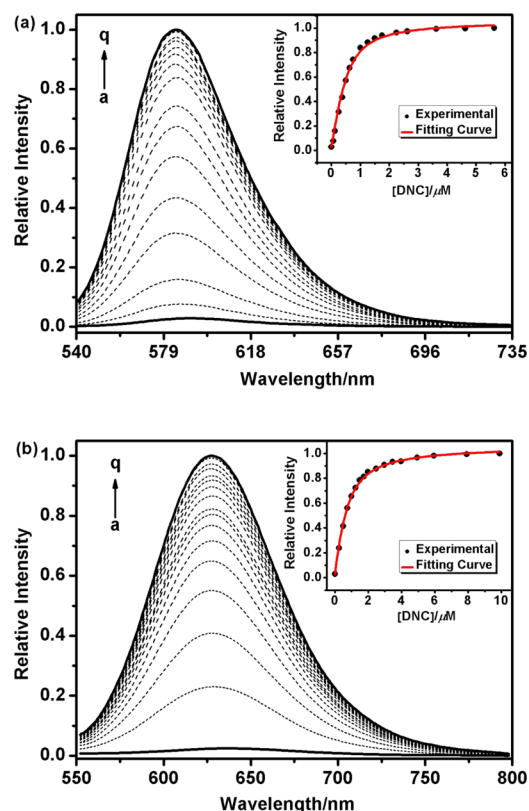


Figure 4. Fluorescence spectral titrations to evaluate the affinity of G2 and G6 to DNC. Fluorescence intensity changes of (a) G2 and (b) G6 upon gradual addition of DNC in water at 25 °C ($[G_2] = 1.0 \times 10^{-6} \text{ M}$ with $[DNC] = 0\text{--}5.8 \times 10^{-6} \text{ M}$ (a) and $[G_6] = 1.0 \times 10^{-6} \text{ M}$ with $[DNC] = 0\text{--}10.0 \times 10^{-6} \text{ M}$ (b), from line a to q). Inset: Nonlinear least-squares analysis of the fluorescence intensity changes to calculate the 1:1 association constant (*K*).

Microcalorimetric Titration and Thermodynamics. To elucidate the origin of the unprecedented fluorescence enhancement and the extremely strong complexation by such a rather simple host, we evaluated the thermodynamic parameters by means of isothermal titration calorimetry (ITC) and the results were listed in Table 1. The association constants (*K*) obtained by ITC are in good agreement with those obtained by fluorimetric titration mentioned above (Figures S16–S20 in the Supporting Information). Moreover, the electrostatic potential maps also demonstrate that the whole aromatic skeletons in G1, G2, and G4 are very electron-deficient, which is more prone to stack with the π -donor units from the crown ether component (Figure 5). In addition, the peripheral hydrogen atoms around push–pull guest molecules are so acidic (electron-poor) that they can readily form hydrogen-bonding interconnection with the electron-rich oxygen atoms in DNC.^{43,44} Therefore, we can reasonably infer that the π -stacking and hydrogen-bonding interactions are jointly contributed to the enthalpic gains in the present molecular binding system. Along with the dominant enthalpic gains, the moderate entropic changes further confirm that the mutual electrostatic desolvation effect is another primary determinant to govern the molecular recognition process in water, because lacking sulfonated groups, the complexation of organic cations with neutral crown ether derivatives always induces much more negative entropic loss in nonaqueous solvent.⁴⁵

Table 1. Association Constants (K/M^{-1}), Standard Free Energy ($\Delta G^\circ/kJ\cdot mol^{-1}$), Enthalpy ($\Delta H^\circ/kJ\cdot mol^{-1}$), and Entropy Changes ($T\Delta S^\circ/kJ\cdot mol^{-1}$) for 1:1 Inclusion Complexation of DNC with Push–Pull Guests in Water at 25 °C

guest	K	$-\Delta G^\circ$	$-\Delta H^\circ$	$T\Delta S^\circ$
G1	$(2.82 \pm 0.21) \times 10^6$	36.81 ± 0.18	35.47 ± 0.05	1.34 ± 0.23
G2	$(4.94 \pm 0.29) \times 10^6$	38.20 ± 0.14	33.38 ± 0.04	4.82 ± 0.18
G3 ^a	4.32×10^6	37.85	41.39	-3.54
G4	$(8.09 \pm 0.09) \times 10^5$	33.72 ± 0.03	39.37 ± 0.37	-5.65 ± 0.39
G5	$(1.64 \pm 0.08) \times 10^6$	35.47 ± 0.12	40.54 ± 0.07	-5.08 ± 0.20
G6	$(1.82 \pm 0.13) \times 10^6$	35.52 ± 0.02	41.42 ± 0.42	-5.89 ± 0.40

^aThe thermodynamic parameters in the G3CDNC complex could not be accurately obtained by ITC method, due to the low water-solubility of G3. Alternatively, the variable-temperature fluorescence titrations were performed to obtain the reliable thermodynamic parameters according to van't Hoff equation (see Figure S21 in the Supporting Information for details).

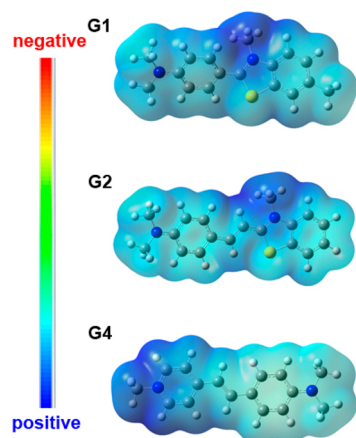


Figure 5. Electrostatic potential surfaces of G1, G2, and G4. Blue and red represent positive and negative electrostatic potentials, respectively.

The calorimetric data in benzothiazolium salt systems clearly indicate that the extraordinarily strong binding of G1–G2 by DNC is driven not only by the highly negative enthalpic change but also by the positive entropic gain. The enthalpic gain may be attributed to the combined effect of the π -stacking, hydrophobic, and hydrogen-bonding interactions, while the favorable entropic gain, which is rarely observed for synthetic host–guest systems, may arise from the extensive dehydration from both the positively charged guests and negatively charged DNC upon charge-neutralizing sandwich complexation, as often observed for biological host–guest systems.^{46,47} The complexation of DNC with G3–G6 is mainly enthalpy-driven with a modest entropic loss, which is an unusual occurrence in the water-soluble crown ether-based molecular recognition systems. The orderly penetrating of stilbazolium salts makes the encapsulated guest molecules more immovable in the crown ether's ring, and this conformational fixation overwhelms the desolvation effect to eventually give unfavorable entropic loss. It is also noted that the intermolecular complexation of DNC with benzothiazolium and stilbazolium salts depends to a large degree on charge distribution. That is, different from the isolated pyridinium terminals in G4–G6, the sulfur atom in G1–G3 could greatly delocalize the charge density on the benzothiazolium skeleton. As a result, the high density of positive charge on *N*-methylated benzothiazole group may facilitate the close contact between the sulfonated anions and quaternary ammonium cations, ultimately giving the positive entropic gain in the G1CDNC and G2CDNC complexes. Meanwhile, the electron-deficient pyridinium terminals in G4–G6 could dramatically reduce the charge density on the whole

molecule, which not only produces a stronger π -stacking communication with electron-rich naphthalenesulfonic moieties to form a tightly packed “sandwich-type” complex but also results in the conformational immobilization upon host–guest complexation.

Quantum Chemical Calculations. After scrutinizing the molecular structures of G1–G6, we may propose two plausible mechanisms for rationalizing the fluorescence enhancement in this host–guest system; (a) the complexation-induced pK_a shift accompanied by the protonation to the electron-donating dimethylaniline nitrogen and (b) the conformational restriction of guest molecules in a specific spatial orientation upon complexation with DNC.^{19,48} As exemplified by thioflavin T (G1), the first mechanism does not appear to operate in our case, since the pH titration experiments demonstrate that both free G1 and G1CDNC complex are protonated only in highly acidic media ($pK_a = 1.05$ and 1.45 , respectively) and free from protonation in the neutral solution employed in this study (Figure S22 in the Supporting Information).

On the other hand, the second mechanism sounds more reasonable, as the photophysical properties of G1 and other representative fluorescent probes are known to be critical functions of the dihedral angle (φ) between the benzothiazole and dimethylaniline planes¹⁸ and the results of our own spectroscopic examinations described above are fully compatible with the sandwich complexation of G1–G6 with DNC. Moreover, it is noteworthy that the mechanism of restriction of intramolecular rotation has been widely accepted and applied in the fabrication of new fluorescent and phosphorescent systems.^{49,50} Therefore, to further explore the influence of conformation restrictions of push–pull guests on the emission properties, G1–G6 were mixed with poly(vinyl alcohol) (PVA) and the mixtures thus obtained were subjected to spin-coating. The spin-coated films were found to exhibit strong and characteristic visible-light emission in the solid state similar to that observed upon encapsulation by DNC in solution, indicative of the conformational fixation of push–pull ligands in the polymer matrix (Figure 6).

To gain further insights into the conformational changes upon complexation of push–pull molecules with DNC, as well as the structural origin of the fluorescence enhancement, quantum chemical calculations were carried out on both free benzothiazolium guests and their DNC-bound complexes in the ground (S_0) and first excited singlet states (S_1).^{51,52} It is documented that the locally excited state of G1 spontaneously relaxes to the twisted intramolecular charge-transfer (TICT) state and hence is rarely fluorescent.⁵³ Our own calculations by the DFT and TDDFT methods revealed that the benzothiazole and aniline moieties of free G1 is not coplanar but twisted by

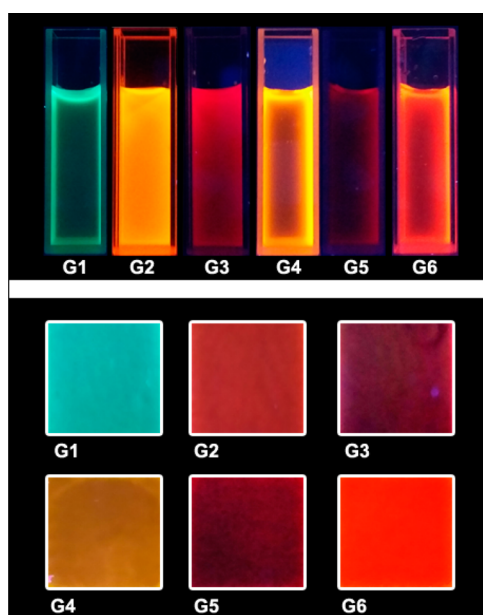


Figure 6. Photographs of (a) the solutions of G1–G6 upon complexation with DNC in water and (b) the spin-coated films of G1–G6 mixed with PVA (5 wt %) irradiated under UV light.

–35.4° even in the ground state (Figure 7a), and the twist angle increases to –69.2° in the excited state (Figure 7c), which is in consistent with the TICT relaxation mechanism.⁵⁴

Intriguingly, photoexcitation induced very contrasting conformational behaviors to free G1 versus G1 in the complex.

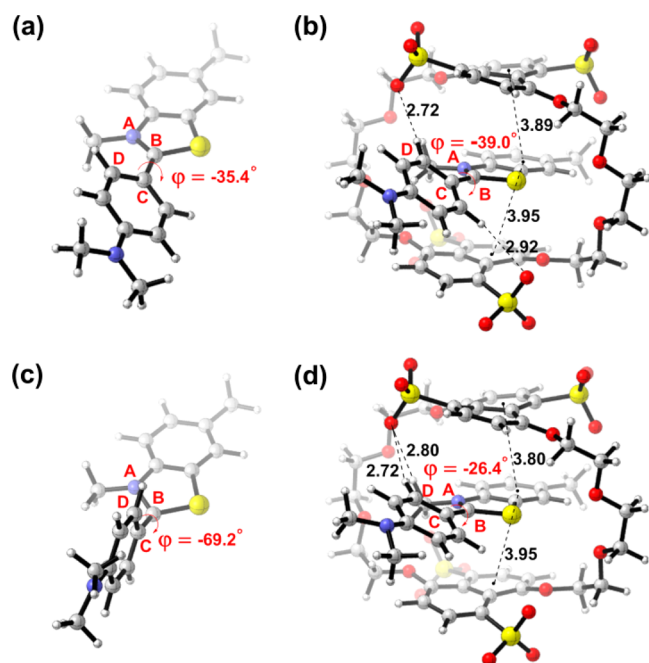
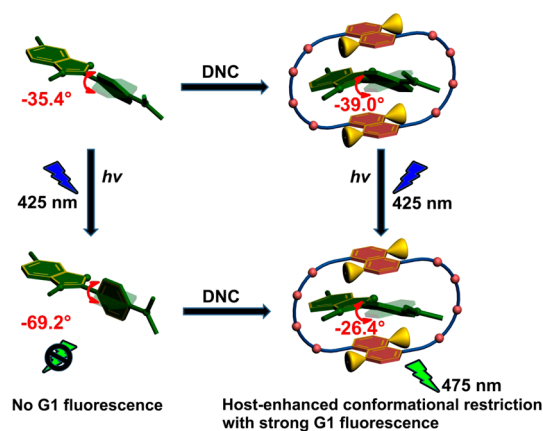


Figure 7. DFT and TDDFT calculations of G1 and G1CDNC complex in the ground and excited states. Optimized geometries for (a, c) free G1 and (b, d) the G1CDNC complex in the (a, b) ground (S_0) and (c, d) first excited singlet (S_1) states in water calculated by the DFT and TDDFT methods, respectively, with the SMD solvation model. The negative dihedral angle represents the clockwise rotation of dimethylaniline ring along the central C_B-C_C bond, relative to the benzothiazole ring.

The inclusion of G1 in DNC cavity merely led to a small increase of the torsion angle from –35.4° to –39.0° (Figure 7b). This result would be somewhat unexpected from the dual π -stacking interactions in the G1CDNC complex. As illustrated in Figure 7b, the G1's benzothiazole is sandwich-complexed by the DNC's naphthalenes in the complex with reasonable interplane distances of 3.89 and 3.95 Å, while the aniline moiety of G1 is not fully accommodated in the DNC cavity and each of the aniline's two *meta* protons are hydrogen-bonded to a sulfonate oxygen of DNC located at a distance of 2.70 or 2.92 Å, respectively, which fixes the twist angle at –39.0°. However, the theoretical calculations revealed a completely different conformational behavior of the G1CDNC complex upon excitation. As shown in Figure 7, parts b and d, the torsion angle is *reduced* from –39.0° in the ground state to –26.4° in the excited state, a behavior opposite to the TICT relaxation mechanism, for which the π -stacking and the dual hydrogen-bonding interactions of one of the sulfonate oxygens with the aniline's *meta* proton and also with one of the *N*-methyl protons in the benzothiazole are responsible. Thus, the π -stacking and hydrogen-bonding interactions between G1 and DNC in the complex turned out to play major roles in determining the photophysical properties of G1. By fixing the excited-state structure of G1 in near coplanar conformation, the originally preferred TICT relaxation is essentially prohibited and the emissive path revives to dramatically augment the fluorescence efficiency (Scheme 1).

Scheme 1. Schematic Illustration of the Sandwich-Type Complexation of DNC with G1 and the Conformational Changes in the Ground and Excited States



Similarly, as discerned from Figure S24a, the most stable G2 in the ground state should be in near coplanar conformation with each of the torsion angles φ_{1-4} around 180° (Chart S1 in the Supporting Information), and this optimized geometry is consistent with its observed crystal structure.⁵⁵ Remarkably, when being started from $\varphi_3 = 180^\circ$, the rotation of double bond $C_D=C_E$, leading to the *trans*- and *cis*-conversion of G2, should overcome a high energy barrier of 27.1 kcal·mol^{–1}, which is much higher than the ones required for C_A-C_B , C_C-C_D , and C_E-C_F single bonds. This implies that rotation of the double bond $C_D=C_E$ hardly occurs under a moderate condition (Figure S25 in the Supporting Information). Upon excitation of G2, the energy barriers for the rotation of C_A-C_B and C_C-C_D single bonds greatly decrease to 5.9 and 2.5 kcal·mol^{–1}, respectively, compared to the situation in the ground

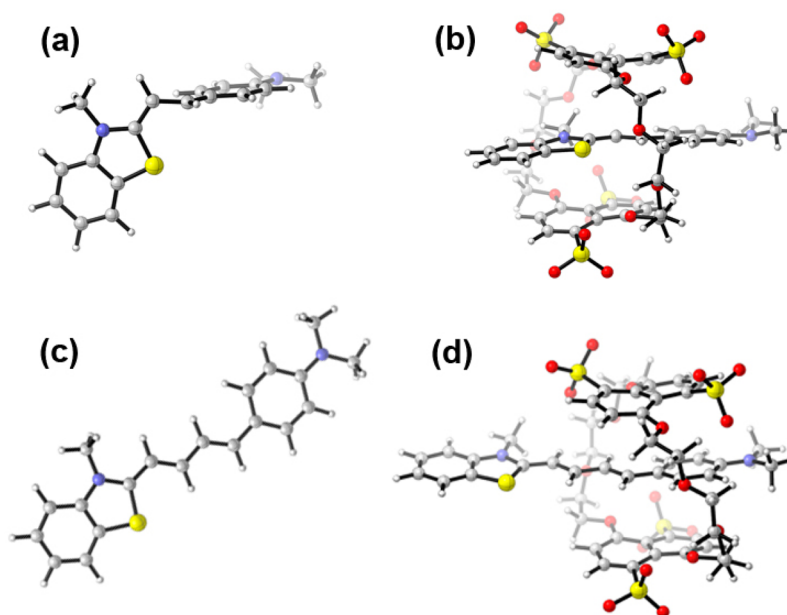


Figure 8. Optimized geometries of (a) G2, (b) G2CDNC complex, (c) G3, and (d) G3CDNC complex in the singlet excited state (S_1) by TDDFT calculation.

state. Moreover, the double bond $C_D=C_E$ can easily rotate with a low energy barrier of $7.7 \text{ kcal}\cdot\text{mol}^{-1}$ in the excited state. Obviously, the free rotation of these chemical bonds can lead to energy dissipation and undesirable fluorescence quenching of G2 in the excited state. Moreover, the dual rotation of single bond C_C-C_D and double bond $C_D=C_E$ gives a more stable conformation at $\varphi_2 = \varphi_3 = 90^\circ$. These results indicate that in the first excited state, the highly twisted conformation of G2 is more favorable than its coplanar one, and the TICT relaxation via these twisted conformations also lead to nonradiative deactivation process (Figures 8a and S26 in the Supporting Information). Significantly, although the rotation of C_C-C_F bonds can easily take place upon excitation, they are inhibited to a large extent by the steric hindrance of DNC. As a result, G2 still adopts the coplanar conformation in the excited G2CDNC complex, by which the TICT relaxation and energy dissipation could be simultaneously suppressed (Figure 8b). Moreover, it is noticed that the dimethylaniline group is located outside DNC, but the twisted intermediate of $\varphi_1 = 90^\circ$ resulting from the C_A-C_B bond rotation is less stable than the coplanar conformation ($\varphi_1 = 0^\circ$ or 180°) by $2.6 \text{ kcal}\cdot\text{mol}^{-1}$ of energy barrier. Therefore, the twisted conformation and TICT relaxation cannot occur via the rotation of the C_A-C_B bond even though the dimethylaniline group of G2 is located outside DNC.

Interestingly, the quantum chemical calculations demonstrate that the binding mechanism in the G3CDNC complexes is somewhat different from the one in the G1CDNC and G2CDNC complexes.⁵⁶ The coplanar structure is the most stable conformation of G3 with each torsion angle φ_{1-6} around 180° in the ground state (Figures S24c and S27 in the Supporting Information), and the rotation of $C_D=C_E$ and $C_F=C_G$ double bonds should overcome high energy barriers of 26.3 and $25.5 \text{ kcal}\cdot\text{mol}^{-1}$, respectively. As compared to the ground state, the energy barriers for bond rotation sharply decrease in the singlet excited state and particularly, the $C_D=C_E$ and $C_F=C_G$ double bonds can freely rotate with relatively low energy barriers of 7.7 and $10.8 \text{ kcal}\cdot\text{mol}^{-1}$, respectively

(Figure S28 in the Supporting Information). These results definitely confirm that the nonradiative decay may occur via more flexible conformation in the excited G3 and thus give a rather lower fluorescence intensity. Different from G2, the twisted intermediate located at $\varphi_{2-5} = 90^\circ$ is less stable than the coplanar isomer ($\varphi = 180^\circ$) and the coplanar G3 is the dominant species in the excited state (Figure 8c). Nevertheless, the encapsulation with DNC can greatly hinder the rotation of central bonds in G3 and force to be accommodated in the DNC's cavity as coplanar conformation upon excitation (Figure 8d). It is also found that instead of dimethylaniline group, the benzothiazole part moved out of the crown ether's ring, probably due to the increased hydrophobic area by elongating the π -conjugation spacer. However, the energy barrier for C_G-C_H bond rotation at $\varphi_6 = 90^\circ$ reaches up to $14.4 \text{ kcal}\cdot\text{mol}^{-1}$ upon excitation, reflecting that the rotation of this bond is fairly difficult to take place under the experimental condition (Figure S28d in the Supporting Information). Therefore, due to the steric hindrance and high rotational energy barriers, the excited G3 in the DNC's cavity maintains the rigidified coplanar conformation, which is responsible for the complexation-induced fluorescence enhancement. Overall, the spatially rigid organization by water-soluble crown ether is of critical importance in regulating the fluorescence emission behaviors of the examined push-pull molecules.

CONCLUSION

In conclusion, the intrinsically hydrophobic cavity of DNC, possessing abundant anchoring points, can be utilized as an artificial receptor to simulate the biological receptors in a much simpler and convenient manner. With the aid of positive supramolecular cooperativity, the inclusion complexation with DNC can dynamically modulate the photophysical behaviors of various push-pull molecules to extraordinarily enhance the fluorescence intensity to the level of receptor-ligand association in the biological system. As demonstrated by the spectroscopic and computer simulation studies, the high-level affinity and the host-assisted conformational fixation are the

essential factors that dramatically enhance the fluorescence efficiency, which may lead us to a simple and straightforward way to elucidate the general binding mechanism operative in the specific recognition process. This finding also promotes the use of DNC as a model host for mimicking and investigating the complexation behaviors of other receptor–ligand binding systems and stimulates the mechanistic study in molecular detail. We also envision that, besides the commonly employed pyridinium and other electron-deficient guests, the push–pull molecules can be utilized as an ideal candidate in the complexation with water-soluble crown ethers, because such type of ligands gathers the structural advantages of positively charged center and π -conjugated skeleton, which are the intrinsic characteristics for strong electrostatic and π -stacking interactions in the pursuit of controlled photophysical properties. Further studies on the complexation of water-soluble crown ether with other functional dipolar push–pull ligands are currently in progress.

■ ASSOCIATED CONTENT

■ Supporting Information

The Supporting Information is available free of charge on the ACS Publications website at DOI: 10.1021/acs.jpcc.6b02646.

Additional UV/vis absorption, fluorescence, and 2D NMR spectra, and Job's plot, as well as the detailed quantum mechanical calculation results (PDF)

■ AUTHOR INFORMATION

Corresponding Author

* (Y.L.) E-mail: yuliu@nankai.edu.cn. Telephone/Fax: +86-22-23503625.

Notes

The authors declare no competing financial interest.

■ ACKNOWLEDGMENTS

We thank the National Natural Science Foundation of China (Nos. 21432004, 21472100, and 91527301) for financial support.

■ REFERENCES

- (1) Onufriev, A. V.; Alexov, E. Protonation and pK Changes in Protein–Ligand Binding. *Q. Rev. Biophys.* **2013**, *46*, 181–209.
- (2) Petukh, M.; Stefl, S.; Alexov, E. The Role of Protonation States in Ligand–Receptor Recognition and Binding. *Curr. Pharm. Des.* **2013**, *19*, 4182–4190.
- (3) Lensink, M. F.; Méndez, R. Recognition-induced Conformational Changes in Protein–Protein Docking. *Curr. Pharm. Biotechnol.* **2008**, *9*, 77–86.
- (4) van der Horst, M. A.; Hellingwerf, K. J. Photoreceptor Proteins, “Star Actors of Modern Times”: A Review of the Functional Dynamics in the Structure of Representative Members of Six Different Photoreceptor Families. *Acc. Chem. Res.* **2004**, *37*, 13–20.
- (5) Boggio-Pasqua, M.; Robb, M. A.; Groenhof, G. Hydrogen Bonding Controls Excited-State Decay of the Photoactive Yellow Protein Chromophore. *J. Am. Chem. Soc.* **2009**, *131*, 13580–13581.
- (6) Koshland, D. E. Application of A Theory of Enzyme Specificity to Protein Synthesis. *Proc. Natl. Acad. Sci. U. S. A.* **1958**, *44*, 98–104.
- (7) Koshland, D. E. The Key–lock Theory And the Induced Fit Theory. *Angew. Chem., Int. Ed. Engl.* **1995**, *33*, 2375–2378.
- (8) Shi, B.; Jie, K.; Zhou, Y.; Zhou, J.; Xia, D.; Huang, F. Nanoparticles with Near-Infrared Emission Enhanced by Pillararene-Based Molecular Recognition in Water. *J. Am. Chem. Soc.* **2016**, *138*, 80–83.
- (9) Peters, G. M.; Skala, L. P.; Davis, J. T. A Molecular Chaperone for G4-Quartet Hydrogels. *J. Am. Chem. Soc.* **2016**, *138*, 134–139.
- (10) Guan, W.; Zhou, W.; Lu, C.; Tang, B. Z. Synthesis and Design of Aggregation-Induced Emission Surfactants: Direct Observation of Micelle Transitions and Microemulsion Droplets. *Angew. Chem., Int. Ed.* **2015**, *54*, 15160–15164.
- (11) Yan, X.; Cook, T. R.; Wang, P.; Huang, F.; Stang, P. J. Highly Emissive Platinum(II) Metallacages. *Nat. Chem.* **2015**, *7*, 342–348.
- (12) Zheng, L.; Sonzini, S.; Ambarwati, M.; Rosta, E.; Scherman, O. A.; Herrmann, A. Turning Cucurbit[8]uril into a Supramolecular Nanoreactor for Asymmetric Catalysis. *Angew. Chem., Int. Ed.* **2015**, *54*, 13007–13011.
- (13) Leitl, M. J.; Krylova, V. A.; Djurovich, P. I.; Thompson, M. E.; Yersin, H. Phosphorescence versus Thermally Activated Delayed Fluorescence. Controlling Singlet–Triplet Splitting in Brightly Emitting and Sublimable Cu(I) Compounds. *J. Am. Chem. Soc.* **2014**, *136*, 16032–16038.
- (14) Freitag, M.; Gundlach, L.; Piotrowiak, P.; Galoppini, E. Fluorescence Enhancement of Di-*p*-tolyl Viologen by Complexation in Cucurbit[7]uril. *J. Am. Chem. Soc.* **2012**, *134*, 3358–3366.
- (15) Groenning, M. Binding Mode of Thioflavin T and Other Molecular Probes in the Context of Amyloid Fibrils—Current Status. *J. Chem. Biol.* **2010**, *3*, 1–18.
- (16) Hawe, A.; Sutter, M.; Jiskoot, W. Extrinsic Fluorescent Dyes as Tools for Protein Characterization. *Pharm. Res.* **2008**, *25*, 1487–1499.
- (17) Biancalana, M.; Koide, S. Molecular Mechanism of Thioflavin-T Binding to Amyloid Fibrils. *Biochim. Biophys. Acta, Proteins Proteomics* **2010**, *1804*, 1405–1412 and references therein..
- (18) Amdursky, N.; Erez, Y.; Huppert, D. Molecular Rotors: What Lies Behind the High Sensitivity of the Thioflavin-T Fluorescent Marker. *Acc. Chem. Res.* **2012**, *45*, 1548–1557.
- (19) Harel, M.; Sonoda, L. K.; Silman, I.; Sussman, J. L.; Rosenberry, T. L. Crystal Structure of Thioflavin T Bound to the Peripheral Site of *Torpedo californica* Acetylcholinesterase Reveals How Thioflavin T Acts as a Sensitive Fluorescent Reporter of Ligand Binding to the Acylation Site. *J. Am. Chem. Soc.* **2008**, *130*, 7856–7861.
- (20) Ajami, D.; Rebek, J., Jr. More Chemistry in Small Spaces. *Acc. Chem. Res.* **2013**, *46*, 990–999.
- (21) Biroš, S. M.; Rebek, J., Jr. Structure and Binding Properties of Water-Soluble Cavitands and Capsules. *Chem. Soc. Rev.* **2007**, *36*, 93–104.
- (22) Ma, X.; Tian, H. Stimuli-responsive Supramolecular Polymers in Aqueous Solution. *Acc. Chem. Res.* **2014**, *47*, 1971–1981.
- (23) Ma, X.; Zhao, Y. Biomedical Applications of Supramolecular Systems Based on Host–Guest Interactions. *Chem. Rev.* **2015**, *115*, 7794–7839.
- (24) Serreli, V.; Lee, C.-F.; Kay, E. R.; Leigh, D. A. A Molecular Information Ratchet. *Nature* **2007**, *445*, 523–527.
- (25) Juriček, M.; Strutt, N. L.; Barnes, J. C.; Butterfield, A. M.; Dale, E. J.; Baldrige, K. K.; Stoddart, J. F.; Siegel, J. S. Induced-fit Catalysis of Corannulene Bowl-to-bowl Inversion. *Nat. Chem.* **2014**, *6*, 222–228.
- (26) Chen, L.; Zhang, Y.-M.; Liu, Y. Molecular Binding Behaviors between Tetrasulfonated Bis(*m*-phenylene)-26-crown-8 and Bispiperidinium Guests in Aqueous Solution. *J. Phys. Chem. B* **2012**, *116*, 9500–9506.
- (27) Chen, L.; Zhang, Y.-M.; Wang, L.-H.; Liu, Y. Molecular Binding Behaviors of Pyromellitic and Naphthalene Diimide Derivatives by Tetrasulfonated 1,5-Dinaphtho-(3n+8)-crown-n (n = 8, 10) in Aqueous Solution. *J. Org. Chem.* **2013**, *78*, 5357–5363.
- (28) Zhang, Y.-M.; Wang, Z.; Chen, L.; Song, H.-B.; Liu, Y. Thermodynamics and Structures of Complexation between Tetrasulfonated 1,5-Dinaphtho-38-crown-10 and Diquaternary Salts in Aqueous Solution. *J. Phys. Chem. B* **2014**, *118*, 2433–2441.
- (29) Rodríguez-Rodríguez, C.; Rimola, A.; Rodríguez-Santiago, L.; Ugliengo, P.; Álvarez-Larena, Á.; Gutiérrez-de-Terán, H.; Sodupe, M.; González-Duarte, P. Crystal Structure of Thioflavin-T and Its Binding to Amyloid Fibrils: Insights at the Molecular Level. *Chem. Commun.* **2010**, *46*, 1156–1158.

- (30) Chen, L.; Zhang, H.-Y.; Liu, Y. High Affinity Crown Ether Complexes in Water: Thermodynamic Analysis, Evidence of Crystallography and Binding of NAD⁺. *J. Org. Chem.* **2012**, *77*, 9766–9773.
- (31) Clemo, G. R.; Swan, G. A. The Absorption Spectra of 4-(*p*-Dimethylaminostyryl)pyridine Methiodide and 2:4-Di-(*p*-dimethylaminostyryl)-pyridine Methiodide. *J. Chem. Soc.* **1938**, 1454–1455.
- (32) Sigmundová, I.; Zahradník, P.; Loos, D. Synthesis and Study of Novel Benzothiazole Derivatives with Potential Nonlinear Optical Properties. *Collect. Czech. Chem. Commun.* **2007**, *72*, 1069–1093.
- (33) Retna Raj, C.; Ramaraj, R. Influence of Cyclodextrin Complexation on the Emission of Thioflavin T and its Off-on Control. *J. Photochem. Photobiol., A* **1999**, *122*, 39–46.
- (34) Dutta Choudhury, S.; Mohanty, J.; Upadhyaya, H. P.; Bhasikuttan, A. C.; Pal, H. Photophysical Studies on the Noncovalent Interaction of Thioflavin T with Cucurbit[n]uril Macrocycles. *J. Phys. Chem. B* **2009**, *113*, 1891–1898.
- (35) Zhong, C. The Driving Forces for Twisted or Planar Intramolecular Charge Transfer. *Phys. Chem. Chem. Phys.* **2015**, *17*, 9248–9257.
- (36) Cao, X.; Tolbert, R. W.; McHale, J. L.; Edwards, W. D. Theoretical Study of Solvent Effects on the Intramolecular Charge Transfer of a Hemicyanine Dye. *J. Phys. Chem. A* **1998**, *102*, 2739–2748.
- (37) Strehmel, B.; Seifert, H.; Rettig, W. Photophysical Properties of Fluorescence Probes. 2. A Model of Multiple Fluorescence for Stilbazolium Dyes Studied by Global Analysis and Quantum Chemical Calculations. *J. Phys. Chem. B* **1997**, *101*, 2232–2243.
- (38) Carlotti, B.; Consiglio, G.; Elisei, F.; Fortuna, C. G.; Mazzucato, U.; Spalletti, A. Intramolecular Charge Transfer of Push–Pull Pyridinium Salts in the Triplet Manifold. *J. Phys. Chem. A* **2014**, *118*, 7782–7787.
- (39) Khurana, R.; Coleman, C.; Ionescu-Zanetti, C.; Carter, S. A.; Krishna, V.; Grover, R. K.; Roy, R.; Singh, S. Mechanism of Thioflavin T Binding to Amyloid Fibrils. *J. Struct. Biol.* **2005**, *151*, 229–238.
- (40) Sabaté, R.; Lascu, I.; Saupe, S. J. On the Binding of Thioflavin-T to HET-s Amyloid Fibrils Assembled at pH 2. *J. Struct. Biol.* **2008**, *162*, 387–396.
- (41) Houk, K. N.; Leach, A. G.; Kim, S. P.; Zhang, X. Binding Affinities of Host–Guest, Protein–Ligand, and Protein–Transition-State Complexes. *Angew. Chem., Int. Ed.* **2003**, *42*, 4872–4897.
- (42) Singh, P. K.; Kumbhakar, M.; Pal, H.; Nath, S. Ultrafast Bond Twisting Dynamics in Amyloid Fibril Sensor. *J. Phys. Chem. B* **2010**, *114*, 2541–2546.
- (43) Huang, F.; Switek, K. A.; Zakharov, L. N.; Fronczek, F. R.; Slebodnick, C.; Lam, M.; Golen, J. A.; Bryant, W. S.; Mason, P. E.; Rheingold, A. L.; et al. Bis(*m*-phenylene)-32-crown-10-Based Cryptands, Powerful Hosts for Paraquat Derivatives. *J. Org. Chem.* **2005**, *70*, 3231–3241.
- (44) Liu, Y.; Klivansky, L. M.; Khan, S. I.; Zhang, X. Templated Synthesis of Desymmetrized [2]Catenanes with Excellent Translational Selectivity. *Org. Lett.* **2007**, *9*, 2577–2580.
- (45) Liu, Y.; Li, C.-J.; Zhang, H.-Y.; Wang, L.-H.; Li, X.-Y. Thermodynamics of Complexes between Dibenzo-24-crown-8 Derivatives and 1,2-Bis(pyridinium)ethanes. *Eur. J. Org. Chem.* **2007**, 2007, 4510–4516.
- (46) Inoue, Y.; Wada, T. Molecular recognition in chemistry and biology as viewed from enthalpy–entropy compensation effect. *Advances in Supramolecular Chemistry*; Gokel, G. W., Ed.; JAI Press: Greenwich, CT, 1997; Vol. 4, pp 55–96.
- (47) Rekharsky, M.; Inoue, Y. Solvation effects in supramolecular recognition. *Supramolecular Chemistry: From Molecules to Nanomaterials*; Gale, P. A., Steed, J. W., Eds.; Wiley: Chichester, U.K., 2012; pp 117–133.
- (48) Ghosh, I.; Nau, W. M. The Strategic Use of Supramolecular pKa Shifts to Enhance the Bioavailability of Drugs. *Adv. Drug Delivery Rev.* **2012**, *64*, 764–783.
- (49) Hong, Y.; Lam, J. W. Y.; Tang, B. Z. Aggregation-Induced Emission: Phenomenon, Mechanism and Applications. *Chem. Commun.* **2009**, 4332–4353.
- (50) Ding, D.; Li, K.; Liu, B.; Tang, B. Z. Bioprobes Based on AIE Fluorogens. *Acc. Chem. Res.* **2013**, *46*, 2441–2453.
- (51) Kiss, G.; Çelebi-Ölçüm, N.; Moretti, R.; Baker, D.; Houk, K. N. Computational Enzyme Design. *Angew. Chem., Int. Ed.* **2013**, *52*, 5700–5725.
- (52) Liu, F.; Wang, H.; Houk, K. N. Gated Container Molecules. *Sci. China: Chem.* **2011**, *54*, 2038–2044.
- (53) Stsiapura, V. I.; Maskevich, A. A.; Kuzmitsky, V. A.; Turoverov, K. K.; Kuznetsova, I. M. Computational Study of Thioflavin T Torsional Relaxation in the Excited State. *J. Phys. Chem. A* **2007**, *111*, 4829–4835.
- (54) It should be mentioned here that an alternative conformation with a torsion angle of + 35.4° was also obtained in the calculation (Figure S23 in the Supporting Information).
- (55) Coe, B. J.; Harris, J. A.; Hall, J. J.; Brunchwitz, B. S.; Hung, S.-T.; Libaers, W.; Clays, K.; Coles, S. J.; Horton, P. N.; Light, M. E.; et al. Syntheses and Quadratic Nonlinear Optical Properties of Salts Containing Benzothiazolium Electron-Acceptor Groups. *Chem. Mater.* **2006**, *18*, 5907–5918.
- (56) Miao, J.-T.; Fan, C.; Sun, R.; Xu, Y.-J.; Ge, J.-F. Optical Properties of Hemicyanines with Terminal Amino Groups and Their Applications in Near-infrared Fluorescent Imaging of Nucleoli. *J. Mater. Chem. B* **2014**, *2*, 7065–7072.